Edinburgh, Scotland
EURONOISE 2009
October 26-28

Numerical calculation of pressure modes at high frequencies in lined ducts with a shear flow

O. Olivieri *
A. McAlpine
R. J. Astley
Institute of Sound and Vibration Research
University of Southampton
Southampton, SO17 1BJ, U.K.

ABSTRACT

This paper describes an implementation of the standard Galerkin finite element method for the analysis of the acoustic and vortical modes in an axisymmetric lined duct carrying a high speed, subsonic, parallel mean shear flow. This is fundamentally theoretical work, but with a view to the specific engineering application of acoustic liner optimization in turbofan aero-engine ducts, as cylindrical and annular ducts are approximate models of inlet and bypass ducts, respectively. At high frequencies, the acoustic wavelength is comparable to the boundary layer thickness and this has an effect on acoustic refraction close to the duct walls. Preliminary results of this study reveal how different boundary layer profiles affect sound attenuation in a lined duct, compared with a uniform mean flow. The method solves the third-order eigenvalue problem for the pressure perturbation (Pridmore-Brown equation) with a locally reacting impedance boundary condition. The distinctive feature of this implementation is that it is fast and efficient. Owing to the circular geometry, the problem is reduced to a one-dimensional finite element solution, which permits at high frequencies the calculation of a large number of modes at a modest computational cost.

1 INTRODUCTION

In modern high-bypass-ratio turbofan aero-engines, fan noise is among the most important sources of aircraft noise. Sound due to the fan, such as rotor-stator interaction tones, propagates through the inlet and bypass ducts, where acoustic treatment has proved to be an effective means of reducing the sound prior to being radiated into the free field. However, for an optimal choice of acoustic lining some theoretical understanding of the propagation characteristics as a result of the non-uniformity of the flow will provide additional insight. In 1972 Shankar[1] commented that "In addition to being convected and possibly attenuated at the walls, the sound waves suffer refraction as a result of the non-uniformity of the flow". The effect of refraction is likely to be more significant at high frequencies where the acoustic wavelength is comparable to the boundary-layer thickness. This may affect acoustic refraction close to the duct walls, and hence on the overall attenuation. Since sound propagating in inlet and bypass ducts is primarily generated by the fan blades, it has strong high-frequency content because of the fan's very fast rotation speed. The frequency range of interest contains the blade passing frequency plus a number of harmonics.

*e-mail: oo@isvr.soton.ac.uk

It is often assumed that the unsteady flow in inlet and bypass ducts of turbofan aero-engines can be decomposed into a steady mean-flow component and an unsteady perturbation that is small compared to the mean flow. Utilizing this decomposition, and neglecting the viscous and heat-transfer effects in the fluid yields the unsteady Linearized Euler Equations (LEE), for example see Ref.[2].

For the special case of a flow that is uniform axially and circumferentially, but non-uniform in the radial direction (non-swirling but rotational mean flow), the LEE reduce to a second-order ordinary differential equation[1]

$$(1 - M\lambda)\left[\nabla_\perp^2\psi(\mathbf{r}) + k^2\left[(1 - M\lambda)^2 - \lambda^2\right]\psi(\mathbf{r})\right] + 2\lambda\,\nabla_\perp M \cdot \nabla_\perp\psi(\mathbf{r}) = 0 \qquad \text{in } \Omega\,, \qquad (1)$$

where the 'mode shape' ψ is the transverse component of the pressure perturbation, and Ω denotes the acoustic domain. In equation (1), $\nabla_\perp$ denotes the gradient operator in the transverse plane, $\nabla_\perp^2$ is the two-dimensional Laplacian operator, $\mathbf{r} = \mathbf{r}(x, y)$ is the transverse coordinate[2], $M = M(\mathbf{r})$ is the Mach number, assumed to be a function of the transverse coordinate, and $k = \eta/c$ where η is the source frequency and c is the speed of sound. It is convenient to make use of non-dimensional quantities, such that lengths are scaled by a suitable reference lengthscale L (such as the radius of the cylindrical duct), velocities are scaled by a reference velocity c_r (typically the ambient speed of sound), frequencies are scaled by c_r/L, and pressure perturbations are scaled by $\rho_r c_r^2$ (where ρ_r is the ambient density).

It has been assumed that the pressure perturbation - as well as any other 'primitive' variables, such as velocity and density - are time-harmonic travelling waves in the axial direction of the flow, expressed in the form

$$p(t, z, \mathbf{r}) = e^{\mathrm{j}(\eta t - \lambda k z)}\psi(\mathbf{r})\,. \qquad (2)$$

The parameter $\lambda = k_z/k$ is referred to as the *axial propagation constant*, since its imaginary part controls the attenuation of the disturbance in the axial direction.

Imposing Myers[4] locally-reacting impedance boundary condition at the duct walls gives,

$$\mathbf{n} \cdot \nabla_\perp\psi + \frac{\mathrm{j}\,k}{Z_{\text{spec.}}}(1 - M\lambda)^2\psi = 0 \qquad \text{on } \partial\Omega\,, \qquad (3)$$

where $\partial\Omega$ denotes the surface of the acoustic domain, and $Z_{\text{spec.}}$ is the non-dimensional specific acoustic impedance (normalized by $\rho_r c_r$). Equations (1) and (3) represent a third-order eigenvalue problem with eigenvalue λ and eigenfunction ψ. The problem is linear, but has variable coefficients, and does not permit an analytic solution for a general flow profile $M(\mathbf{r})$. Moreover, the eigenvalue appears in the boundary condition.

In this paper there is a brief description of an implementation of the standard Galerkin finite element method which has been used to solve this eigenvalue problem. The method provides a discrete set of eigenmodes, some of which may be classified as acoustic modes, whilst others are non-acoustic perturbations convected with the mean flow which are classified as vortical modes. Since the mean flow is rotational, the acoustic and vortical disturbances are not decoupled as is the case when the flow is uniform.

The objective of this paper is to provide solutions to the eigenvalue problem by using the finite element method. These solutions are the pressure modes in an annular lined duct containing a

[1] This is referred to as the Pridmore-Brown equation, even though the equation derived by Pridmore-Brown in his classic paper[3] describes the behaviour of the pressure perturbation in the special case of a shear flow contained between two infinite plates. The expression given here holds for flows in axially uniform ducts with arbitrary cross-section.

[2] This is an arbitrary function of the rectangular coordinates x and y perpendicular to the duct axis which is aligned with $\hat{\mathbf{z}}$. For example, for a cylindrical duct $r^2 = x^2 + y^2$.

sheared mean flow. The numerical scheme is outlined briefly in Section 2. Then in Section 3 the implementation is validated by comparing with the previous results in Refs.[5,6]. Preliminary results are presented in Section 4. These include comparison of the pressure modes for a number of different flow profiles at a moderately high Helmholtz number k. These results indicate how different boundary-layer profiles may affect sound transmission in a straight annular duct, compared with a uniform mean-flow.

2 FORMULATION OF THE METHOD

Recasting equation (1) subject to boundary condition (3) in weak form is the basis for implementing the Galerkin finite element method utilized in this work. The weak form is expressed in the form

$$\int_\Omega (1-M\lambda)\left\{k^2\left[(1-M\lambda)^2-\lambda^2\right]f^\star\psi-\nabla_\perp f^\star\cdot\nabla_\perp\psi\right\}\,\mathrm{d}\Omega \\ +\int_\Omega 3\lambda f^\star\nabla_\perp M\cdot\nabla_\perp\psi\,\mathrm{d}\Omega\;-\oint_{\partial\Omega}\mathrm{j}\,kA(1-M\lambda)^3 f^\star\psi\,\mathrm{d}\Gamma\;=0 \quad (4)$$

where f is a trial function, * denotes complex conjugate, and $A=1/Z_{\text{spec.}}$ is the specific acoustic admittance at the boundary.

To extract a discrete spectrum of modal solutions from the weak form of the problem, an approximate solution $\hat{\psi}$ is defined. This is expressed in the form

$$\hat{\psi}(\mathbf{r})=\sum_{j=1}^{N}N_j(\mathbf{r})\psi_j\,, \quad (5)$$

where $\psi_j=\psi(\mathbf{r}_j)$ are the values of the solution at the N nodes of an arbitrary mesh spanning the domain Ω, and $N_j(\mathbf{r})$ are global shape functions.

Substituting (5) into (4), and replacing f with in turn each of the N global interpolation functions N_i, and after a lengthy derivation which is not included here, an algebraic eigenvalue problem for λ is obtained, expressed compactly in the form

$$\mathbf{C}(\lambda)\boldsymbol{\psi}=0\,. \quad (6)$$

The matrix $\mathbf{C}(\lambda)$ is an N by N matrix polynomial defined as

$$\mathbf{C}(\lambda)=\sum_{n=0}^{3}\lambda^n\mathbf{C}_n\,, \quad (7)$$

and $\boldsymbol{\psi}$ is the vector

$$\boldsymbol{\psi}=[\psi_1,\psi_2,\ldots\psi_N]^T\,.$$

Also $\mathbf{C}_k$ are square N by N matrices defined as

$$\mathbf{C}_0=k^2\mathbf{M}^{(0)}-\mathbf{K}^{(0)}-\mathrm{j}\,k\,\mathbf{Z}^{(0)}, \qquad \mathbf{C}_1=-3\,k^2\mathbf{M}^{(1)}+\mathbf{K}^{(1)}+3\,\mathrm{j}\,k\,\mathbf{Z}^{(1)}+3\,\mathbf{S},$$
$$\mathbf{C}_2=k^2\big(3\,\mathbf{M}^{(2)}-\mathbf{M}^{(0)}\big)-3\,\mathrm{j}\,k\,\mathbf{Z}^{(2)}, \qquad \mathbf{C}_3=-k^2\big(\mathbf{M}^{(3)}-\mathbf{M}^{(1)}\big)+\mathrm{j}\,k\,\mathbf{Z}^{(3)}\,,$$

where $\mathbf{M}^{(n)}$, $\mathbf{K}^{(n)}$, $\mathbf{Z}^{(n)}$ and $\mathbf{S}$, for $n=0,1,2,3$, are square N by N matrices which are defined,

in index notation, as

$$M_{ij}^{(n)} = \int_\Omega \left[M(\mathbf{r})\right]^n N_i^* N_j \, \mathrm{d}\Omega \,, \tag{8a}$$

$$K_{ij}^{(n)} = \int_\Omega \left[M(\mathbf{r})\right]^n \nabla_\perp N_i^* \cdot \nabla_\perp N_j \, \mathrm{d}\Omega \,, \tag{8b}$$

$$Z_{ij}^{(n)} = \oint_{\partial\Omega} A \left[M(\mathbf{r})\right]^n N_i^* N_j \, \mathrm{d}\Gamma \,, \tag{8c}$$

$$S_{ij} = \int_\Omega N_i^* \, \nabla_\perp M(\mathbf{r}) \cdot \nabla_\perp N_j \, \mathrm{d}\Omega \,. \tag{8d}$$

This formulation follows the same format prescribed by Gabard and Astley[7].

Since in our case the domain Ω is circular and the problem has rotational symmetry, it is natural to use polar coordinates (r, θ). The approximate solution (5) can then be expanded in a complex Fourier series of the form

$$\hat{\psi}(r, \theta) = \sum_{m=0}^{\infty} e^{-\mathrm{j}m\theta} \hat{\psi}_m(r) \,, \tag{9}$$

where $\hat{\psi}_m(r)$ is the radial component of the pressure perturbation, or mode shape, having azimuthal order equal to m. This is found by replacing $N_j(\mathbf{r})$ with $e^{-\mathrm{j}m\theta}\Phi_j(r)$ in (8), where $\Phi_j(r)$ are the one-dimensional global shape functions which can be easily built using Lagrange interpolation functions. This substitution, for a given value of m, leads to a one-dimensional eigenvalue problem. This dramatically improves the computational efficiency because only a one-dimensional mesh is required, with N nodes at $r = r_j$, $j = 1..N$.

Equation (6) can be expressed as a linear eigenvalue problem of the form

$$\mathbf{A}\mathbf{q} = \lambda \mathbf{B}\mathbf{q} \,, \tag{10}$$

where

$$\mathbf{A} = \begin{bmatrix} \mathbf{0} & \mathbf{I} & \mathbf{0} \\ \mathbf{0} & \mathbf{0} & \mathbf{I} \\ -\mathbf{C}_0 & -\mathbf{C}_1 & -\mathbf{C}_2 \end{bmatrix}, \qquad \mathbf{B} = \begin{bmatrix} \mathbf{I} & \mathbf{0} & \mathbf{0} \\ \mathbf{0} & \mathbf{I} & \mathbf{0} \\ \mathbf{0} & \mathbf{0} & \mathbf{C}_3 \end{bmatrix}, \qquad \mathbf{q} = \begin{bmatrix} \boldsymbol{\psi} \\ \lambda\boldsymbol{\psi} \\ \lambda^2\boldsymbol{\psi} \end{bmatrix}, \tag{11}$$

and $\mathbf{0}$ and $\mathbf{I}$ are the square N by N null and identity matrices, respectively.

This procedure can be used with any arbitrary flow profile $M(r)$. The method described here has been programmed using the C++ programming language and a standard eigensystem package which makes use of the QZ algorithm[8].

3 VALIDATION

In this section, results obtained using the implementation described in Section 2 are compared with some benchmark examples to validate the numerical method.

Figure 1 shows the computed eigenvalues ($\lambda = k_z/k$) for the first twelve acoustic eigenmodes, six in each propagation direction and for azimuthal orders $m = 0$ to 3, for a test case with uniform mean flow with Mach number $M = 0.2$ (in the positive direction), with an annular duct having hub-tip-ratio $h = 0.4$. A mesh consisting of 31 nodes and quadratic elements has been used for the FEM calculation. The nodes per wavelength is 22.3, and the (non-dimensional) element size is 0.02. Results in figure 1(a) are for a rigid duct, and in 1(b) for a lined duct with specific acoustic impedance $Z = 1.5 - 3\mathrm{j}$. In both examples, the computed eigenvalues may be compared with the

'exact' eigenvalues which are also shown plotted in figure 1. The 'exact' eigenvalues may, in these test cases, be determined from a closed-form analytic solution of the convected wave equation, since the mean flow is uniform. The agreement between the numerical and analytical values is excellent.

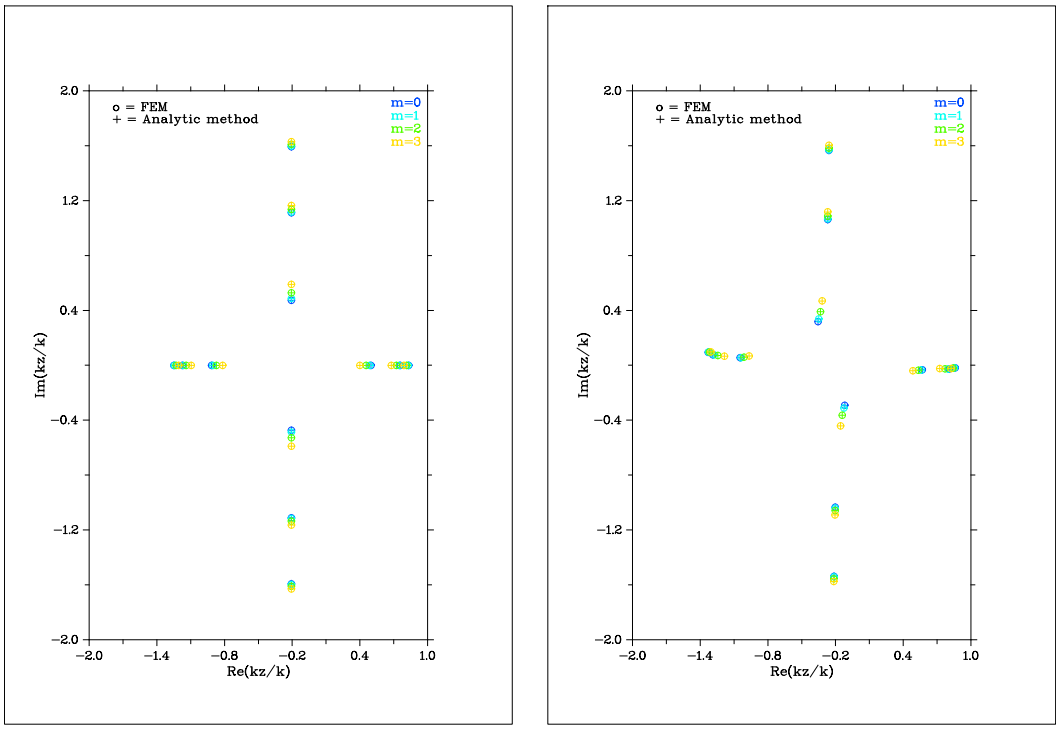

(a) (b)

Figure 1: Comparison between FEM and analytic method. Location of the eigenvalues $\lambda = k_z/k$ in the complex plane: (a) rigid duct; (b) lined duct.

Table 1 and figure 2 contain results for a shear mean flow. In this example the mean flow is not uniform, due to the inclusion of a boundary layer. The variation of the flow velocity is linear through the boundary layer. Eigenmodes corresponding to azimuthal order $m = 1$ only are shown. A mesh consisting of 75 nodes and linear elements has been used for this calculation. The nodes per wavelength is 55, and the (non-dimensional) element size is 0.008. The propagating modes have been ordered according to increasing values of the imaginary part of the wave number, and are compared to the results of Joshi *et al.*[5] and also Brooks[6]. The three sets of results compare well for both upstream and downstream propagating modes.

4 EXAMPLE RESULTS

An annular duct with hub-to-tip ratio $h = 2/3$ is used for the examples in this section. The duct wall is lined having specific acoustic impedance $Z = 2 - 0.5\mathrm{j}$. The frequency corresponds to Helmholtz number $k = 30$. The eigenmodes have been computed for three different mean-flow profiles: (1) Uniform flow; (2) Linear boundary-layer of thickness $\delta = 0.03$; (3) 1/7th power law boundary-layer also of thickness $\delta = 0.03$.

Mode No.	Joshi *et al.*		Brooks		FEM, 75 nodes	
	real	imag	real	imag	real	imag
1+	0.85560	-0.02000	0.85771	-0.02033	0.85831	-0.02008
2+	0.79690	-0.02620	0.80106	-0.02747	0.80140	-0.02710
3+	0.55820	-0.03370	0.56248	-0.03392	0.56139	-0.03369
4+	-0.13080	-0.30470	-0.12450	-0.31137	-0.12799	-0.31059
5+	-0.20000	-1.03670	-0.20534	-1.03813	-0.21349	-1.03934
1-	-1.04080	0.05360	-1.03035	0.05597	-1.03137	0.05691
2-			-1.26632	0.06888	-1.26321	0.06891
3-	-1.32060	0.08010	-1.31128	0.08123	-1.30614	0.08041
4-	-0.35840	0.32790	-0.34621	0.33552	-0.35118	0.33507
5-	-0.28550	1.05930	-0.27248	1.06293	-0.28123	1.06378
6-	-0.28280	1.55780	-0.26602	1.56185	-0.27997	1.56503

Table 1: Eigenvalues $\lambda = k_z/k$ for a lined annular duct with hub-to-tip ratio $h = 0.4$, $m = 1$, $k = 14.06667$, $Z = 1.5 - 3\mathrm{j}$ and a linear boundary-layer flow profile. Outside the boundary layer, $M_0 = 0.2$, whilst the (non-dimensional) boundary-layer thickness $\delta = 0.01$. The FEM results are compared to previous results by Joshi *et al.*[5] and Brooks[6].

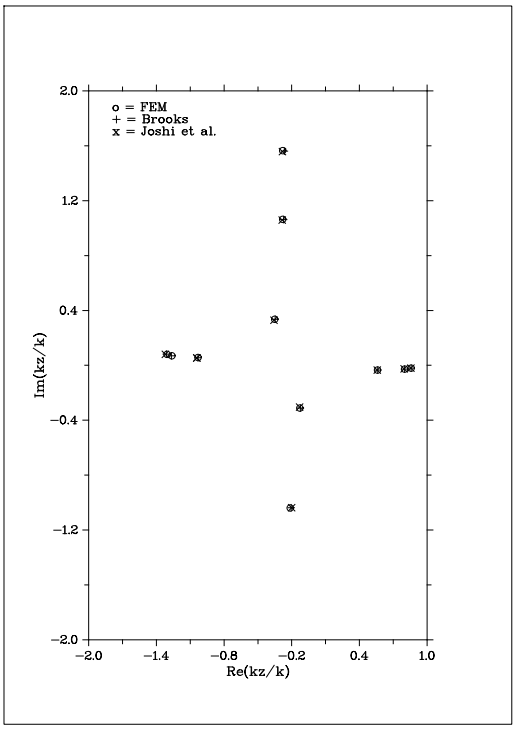

Figure 2: Location of eigenvalues $\lambda = k_z/k$ listed in Table 1 in the complex plane.

Mode No.	Uniform flow		Linear bound. layer		1/7th power law bound. layer	
	real	imag	real	imag	real	imag
1+	0.762254	-0.0298238	0.767216	-0.0429713	0.752477	-0.0385387
2+	0.720099	-0.0666787	0.735697	-0.0857692	0.710757	-0.0959106
3+	0.574907	-0.0867974	0.587065	-0.0985904	0.580324	-0.119471
4+	0.238579	-0.164771	0.236721	-0.176683	0.238334	-0.188594
5+	-0.168087	-0.635233	-0.181914	-0.657412	-0.172457	-0.680591
6+	-0.254177	-1.13849	-0.266665	-1.16711	-0.247567	-1.1805
1-	-1.38066	0.0228141	-1.38276	0.013392	-1.3935	0.0280103
2-	-1.24982	0.120678	-1.25528	0.0746442	-1.31762	0.102902
3-	-1.12519	0.270276	-1.10397	0.184008	-1.19124	0.170892
4-	-0.89105	0.378465	-0.85227	0.288935	-0.891667	0.242585
5-	-0.520351	0.805449	-0.501949	0.725359	-0.498628	0.720267
6-	-0.435734	1.28972	-0.43552	1.19818	-0.432423	1.21014

Table 2: Eigenvalues $\lambda = k_z/k$ for a lined annular duct with hub-to-tip ratio $h = 2/3$, $m = 0$, $k = 30.0$, $Z = 2.0 - 0.5$j and flow profiles: (1) Uniform flow; (2) Linear boundary-layer; (3) 1/7th power law boundary-layer. Outside the boundary layer, $M_0 = 0.3$, whilst the (non-dimensional) boundary-layer thickness $\delta = 0.03$.

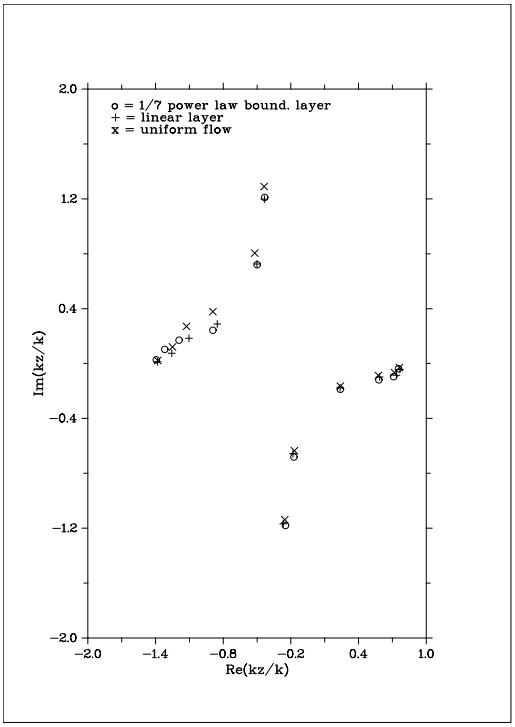

Figure 3: Location of eigenvalues $\lambda = k_z/k$ listed in Table 2 in the complex plane.

The flow profiles for the shear flow test cases are

$$M(r) = \begin{cases} M_0 \left(\dfrac{r-h}{\delta} \right)^{1/N} & h \leqslant r < h+\delta, \\ M_0 & h+\delta \leqslant r \leqslant (1-\delta) \\ M_0 \left(\dfrac{1-r}{\delta} \right)^{1/N} & (1-\delta) < r \leqslant 1 \end{cases} \tag{12}$$

where M_0 is the core flow Mach number, and N defines the power ($N = 1$ for case (2), $N = 7$ for case (3)). In all three cases a one-dimensional mesh consisting of 75 nodes has been used. The nodes per wavelength is 46.5, and the (non-dimensional) element size is 0.0045. Quadratic element shape functions are used for cases (1) and (3) — uniform flow and 1/7th power law boundary layer flow. Linear element shape functions are used for case (2) — linear boundary layer flow.

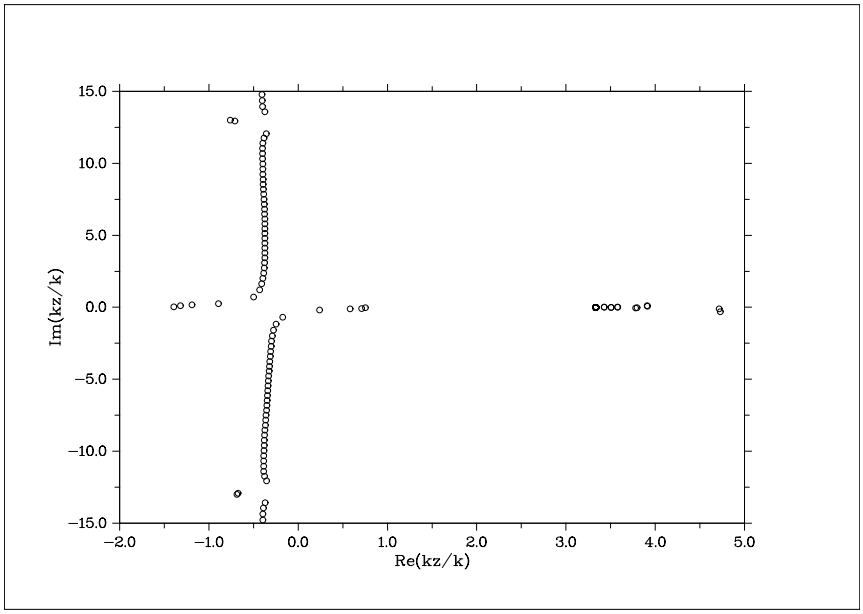

Figure 4: Location of the computed eigenvalues $\lambda = k_z/k$ for the 1/7th power law boundary-layer in the complex plane. The real and positive eigenvalues on the far right of the plot are the vortical modes.

The computed eigenvalues ($\lambda = k_z/k$) for the first twelve acoustic eigenmodes, six in each propagation direction and for azimuthal order $m = 0$, are shown in Table 2 and in Figure 3.

In figure 4 the computed eigenvalues are shown plotted (for the 1/7th power law boundary layer). It is seen that there are two families of acoustic modes (propagating in the positive and negative z-direction). There are also a number of modes which have real and positive eigenvalues. These are identified as being the vortical modes. The number of the latter depend on the number of nodes in the mesh, since the problem has been discretized. In reality the vortical modes constitute a continuous spectrum.

The results illustrate the effect of a boundary layer on sound attenuation compared with a uniform flow. There are small differences in the imaginary part of the axial wave number. The notable differences are for the modes propagating against the flow. Then, generally, with uniform flow the axial decay rates are slightly higher compared to the decay rates with a boundary layer. This is because the sheared flow causes the upstream propagating modes to be refracted towards the centre of the duct, leading to lower pressure at the duct walls. The first radial order, which

typically will be the least attenuated mode, is seen to be the most affected by the type of flow profile, as shown in figure 5 where a selection of mode shapes are plotted. This is significant for noise control because it is the least attenuated mode. Higher radial orders appear less affected by a boundary layer.

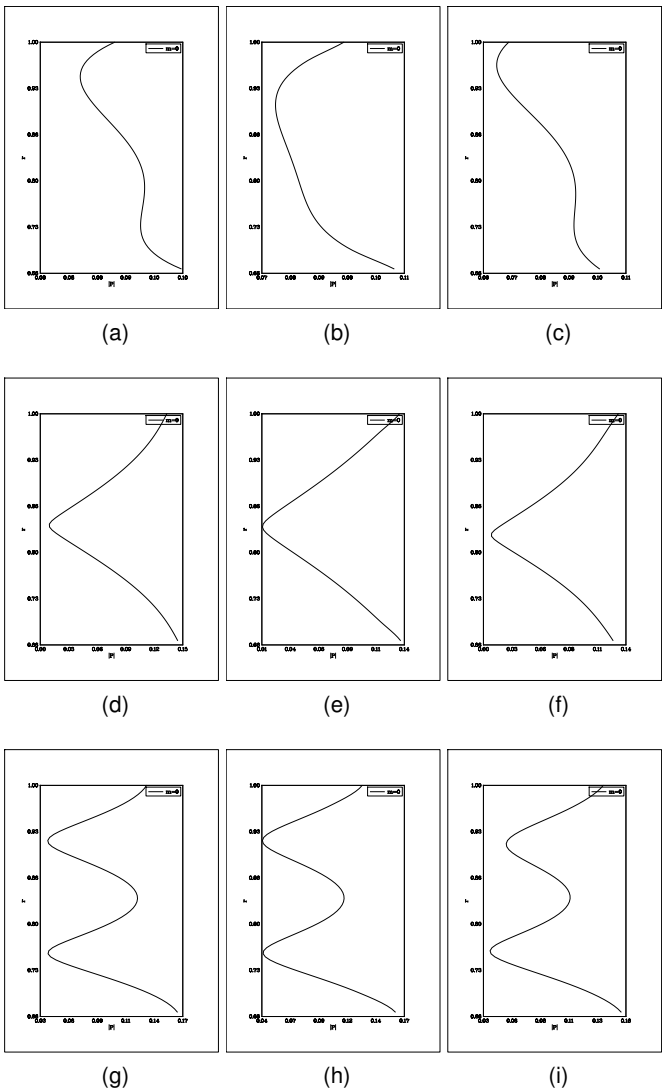

Figure 5: Examples of pressure modeshapes: (1) Uniform flow (a),(d) and (g); (2) Linear boundary-layer (b), (e) and (h); (3) 1/7th power law boundary-layer (c), (f) and (i). Also note that the first radial order are (a-c), the second radial order are (d-f), and the third radial order are (g-i).

5 CONCLUSION

A preliminary study using the Galerkin finite element method to determine the pressure modes in a lined annular duct with sheared mean flow is reported in this paper. The aim is to compute the modes at high frequencies, which is feasible solving the Pridmore-Brown equation using the implementation of the finite element method reported here, because owing to the axisymmetric geometry and mean flow, only a one-dimensional mesh is required allowing, in principle, the calculation of eigenmodes at high frequencies to be determined in a fast and efficient manner.

The numerical method has been validated by comparison of the eigenmodes with 'exact' analytic solutions in the case of a uniform mean flow, and other solutions reported previously in the case of a boundary-layer flow. Also example results showing the eigenmodes, at a moderately high frequency, for three different mean-flow profiles, have been presented. The test cases are uniform flow and shear flows with linear and 1/7th power law boundary-layer profiles. These type of results can be used to examine how the flow profile affects sound attenuation via refraction. This depends on the direction of sound propagation, which may cause refraction of high-frequency sound towards or away from the acoustic lining on the duct walls.

We plan to examine how the boundary-layer flow profile affects the pressure modes at high frequencies. Of key interest is whether boundary layers with similar shape factor (ratio of displacement to momentum thickness) are predicted to have similar pressure modes at high frequencies and, in particular, whether the attenuation determined by the axial decay rates $\mathrm{Im}(\lambda)$ of these modes are comparable.

ACKNOWLEDGMENTS

The first author is supported by an EPSRC grant no. EP/E065775/1. The second and third authors wish to acknowledge the continuing financial support provided by Rolls-Royce plc.

REFERENCES

1. P. N. Shankar. Acoustic Refraction and Attenuation in Cylindrical and Annular Ducts. *Journal of Sound and Vibration*, 22(2):233–&, 1972. ISSN 0022-460X.

2. K. C. Hall and E. F. Crawley. Calculation of Unsteady Flows in Turbomachinery Using the Linearized Euler Equations. *AIAA Journal*, 27(6):777–787, JUN 1989. ISSN 0001-1452.

3. D. C. Pridmore-Brown. Sound Propagation in a Fluid Flowing Through an Attenuating Duct. *Journal of Fluid Mechanics Digital Archive*, 4:393–406, 1958. doi: 10.1017/S0022112058000537.

4. M. K. Myers. On the Acoustic Boundary-Condition in the Presence of Flow. *Journal of Sound and Vibration*, 71(3):429–434, 1980. ISSN 0022-460x.

5. M. C. Joshi, R. E. Kraft, and S. Y. Son. Analysis of sound propagation in annular ducts with segmented treatment and sheared flow. In *AIAA 20th Aerospace Sciences Meeting, January 11-14, Orlando, Florida*. American Institute of Aeronautics and Astronautics, 1982.

6. C. J. Brooks. Prediction and control of sound propagation in turbofan engine bypass ducts, 2007. Eng.D. Thesis, Institute of Sound and Vibration Research, University of Southampton.

7. G. Gabard and R. J. Astley. A Computational Mode-Matching Approach for Sound Propagation in Three-Dimensional Ducts with Flow. *Journal of Sound and Vibration*, 315(4-5):1103–1124, Sep 9 2008. ISSN 0022-460x. doi: 10.1016/J.Jsv.2008.02.015.

8. *IMSL C Numerical Library, Volume 1: C Math Library User's Guide*. Visual Numerics Inc., version 6.0 edition, 2006.